



# Extracellular vesicles derived from breast cancer cells rich in miR-23b-3p, miR-126-3p, and GAS5 inhibited the tumor growth of zebrafish xenograft model

Iulia Andreea Pelisenco<sup>1</sup>, Ilaria Grossi<sup>1</sup>, Daniela Zizioli<sup>1</sup>, Flora Guerra<sup>2</sup>, Cecilia Bucci<sup>2</sup>, Luca Mignani<sup>1</sup>, Giulia Girolimetti<sup>2</sup>, Riccardo Di Corato<sup>3,4</sup>, Vito Giuseppe D'Agostino<sup>5</sup>, Eleonora Marchina<sup>1</sup>, Giuseppina De Petro<sup>1</sup>, Alessandro Salvi<sup>1</sup>

<sup>1</sup> Dept of Molecular and Translational Medicine, Brescia Univ., Brescia, Italy; <sup>2</sup> Dept of Biological and Environmental Sciences and Technologies, Salento Univ., Lecce, Italy; <sup>3</sup> Institute for Microelectronics and Microsystems (IMM), CNR, Lecce, Italy; <sup>4</sup> Center for Biomolecular Nanotechnologies, Istituto Italiano di Tecnologia, Lecce, Italy; <sup>5</sup> Dept of Cellular, Computational and Integrative Biology (CIBIO), Trento University, Trento, Italy

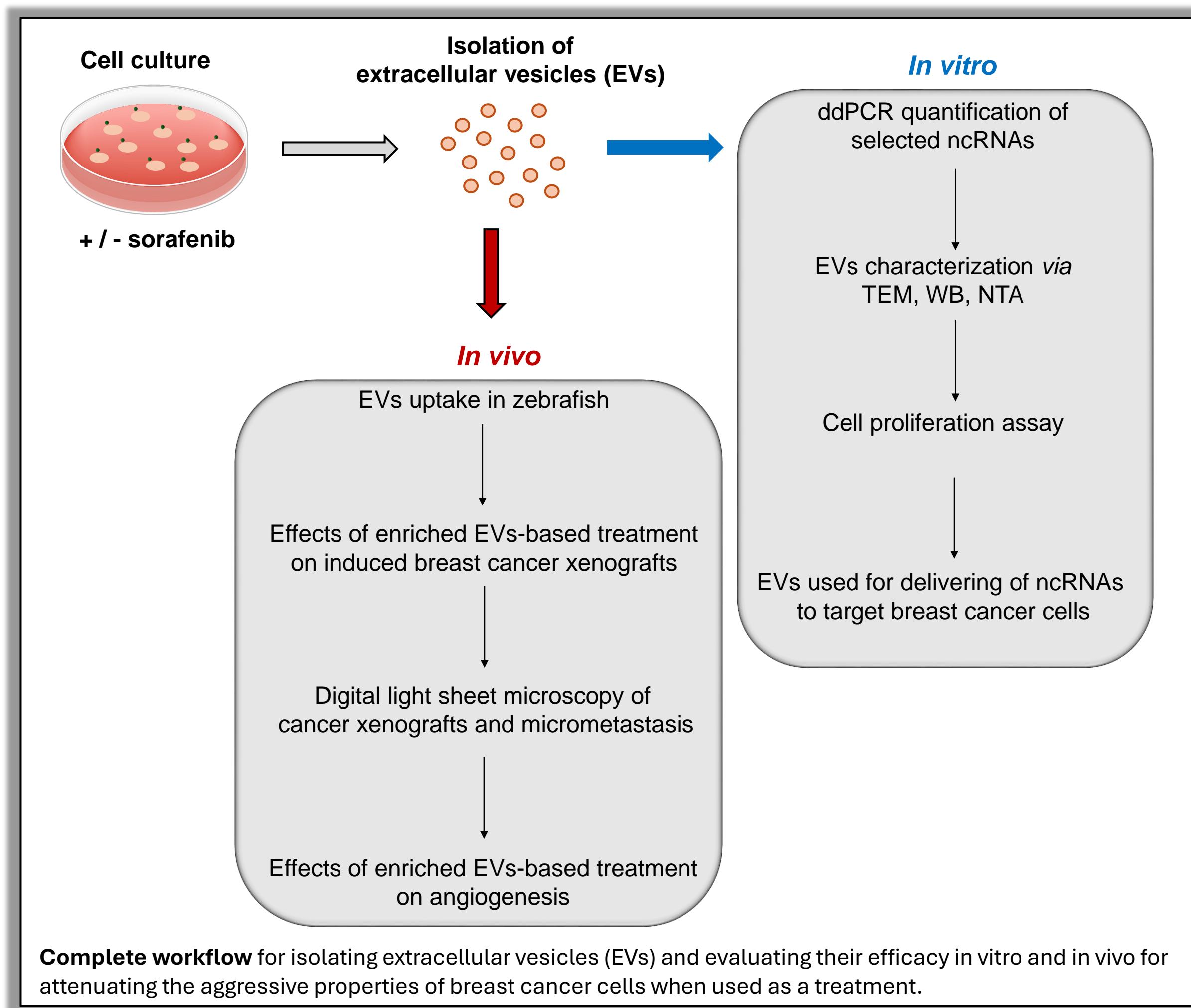
## Background

1

**Extracellular vesicles (EVs)** are cell-derived membranous structures secreted by all cell types. EVs as a mimic of “nature’s delivery system” can be used to **transport nucleic acids, peptides, lipids, and metabolites** to recipient cells for intercellular communication.

## Workflow

2



## Conclusions

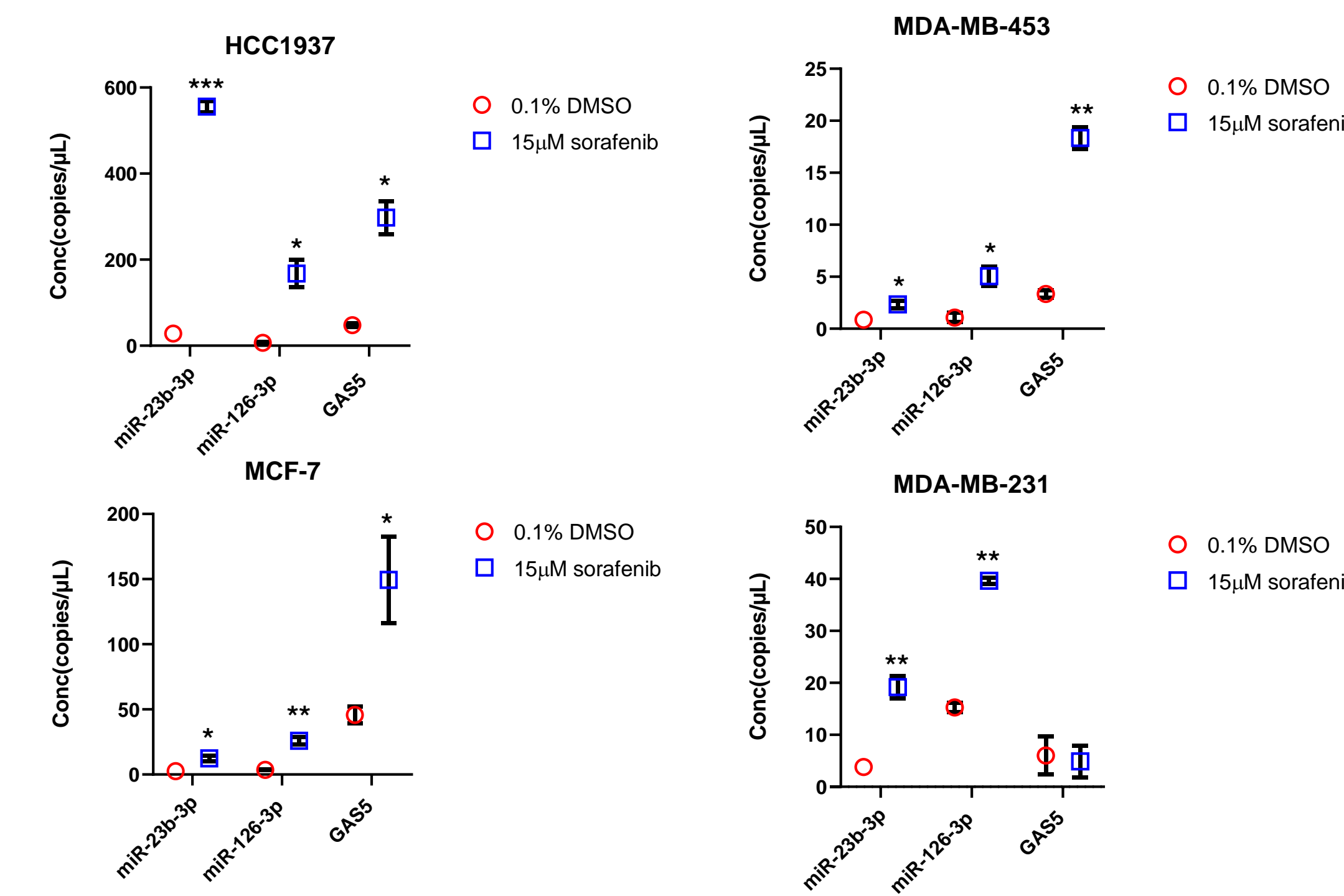
4

Due to their favorable physiological attributes, including **biocompatibility, minimal toxicity, and enhanced stability** within organisms, **EVs** can serve as highly **effective carriers** for a variety of therapeutic compounds, including nucleic acids. Our findings indicate a new way to selectively enrich EVs; the great potential of EVs as **vehicles for ncRNAs**; the combined role of **miR-23b-3p, miR-126-3p, and GAS5** in limiting the aggressive properties of breast cancer *in vitro* and *in vivo*.

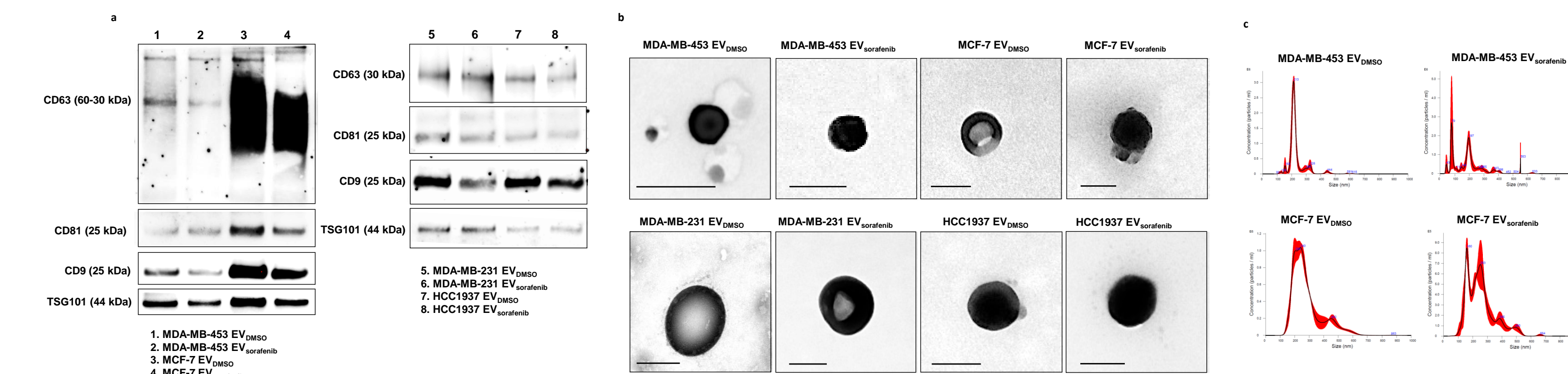
## Results

3

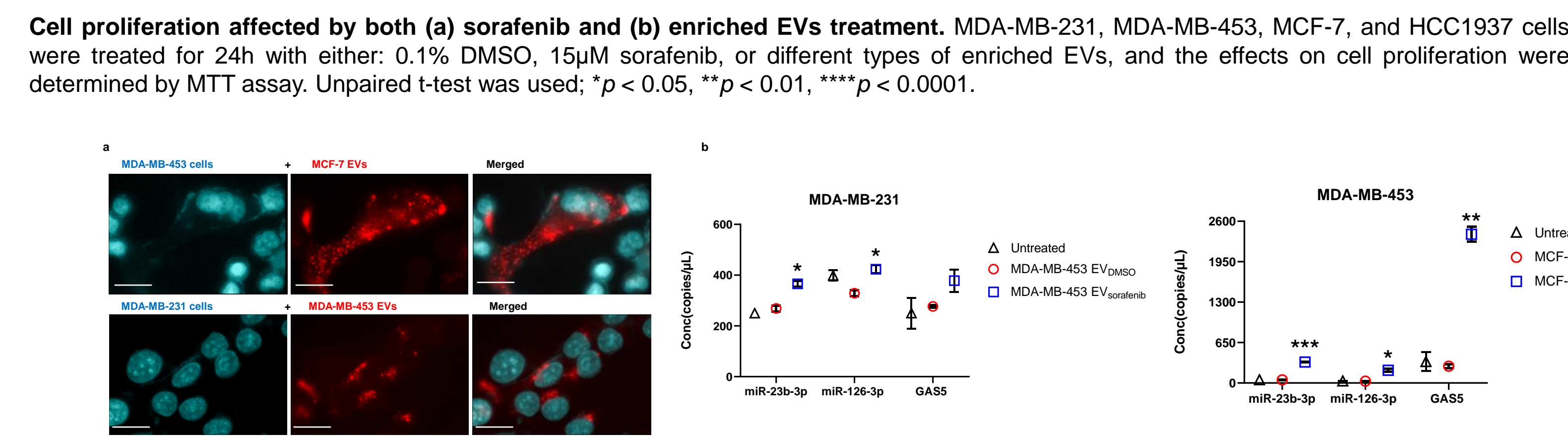
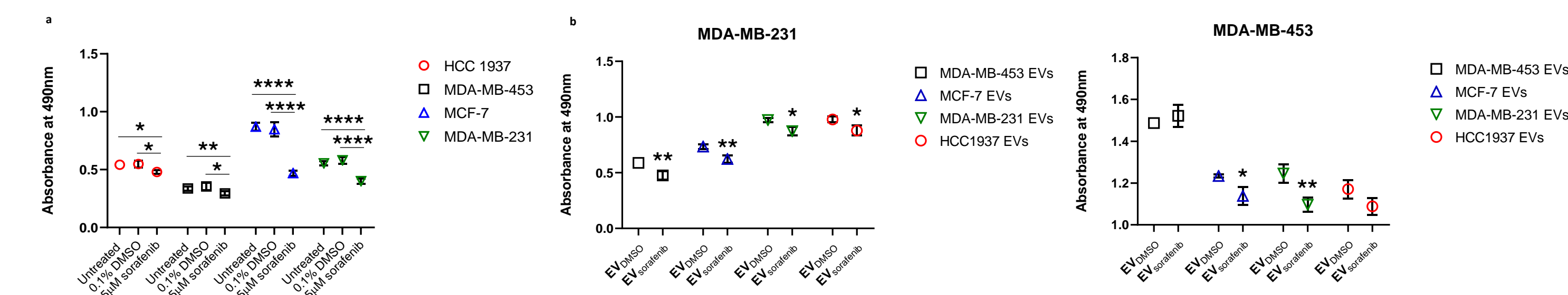
### In vitro



Levels of miR-23b-3p, miR-126-3p, and GAS5 in EVs derived from HCC1937, MDA-MB-453, MCF-7, and MDA-MB-231 breast cancer cells after sorafenib treatment using ddPCR technology. Concentration of each target is expressed as copies/μL; The graphics represent mean value; bars, SD. Unpaired t-test was used; \**p* < 0.05, \*\**p* < 0.01, \*\*\**p* < 0.001.

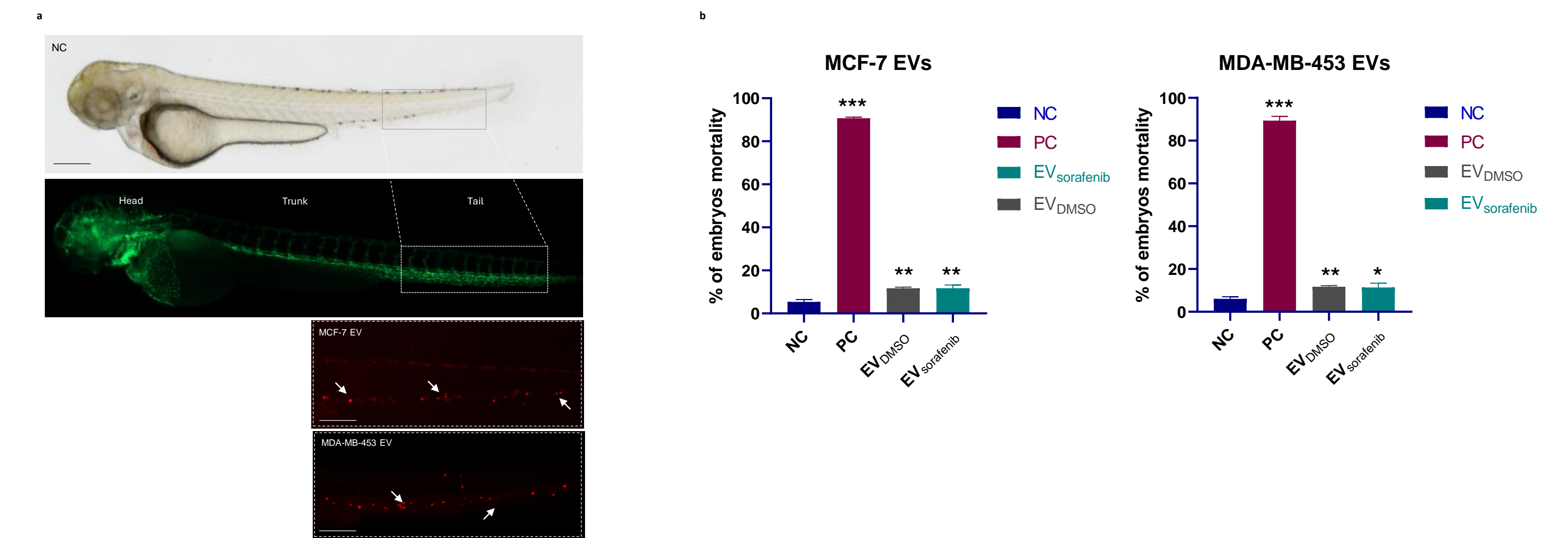


**Characterization of the EVs.** **a** Western blot for tetraspanins (CD63, CD81, CD9) and TSG101 was performed on EVs derived from MDA-MB-453, MCF-7, MDA-MB-231, and HCC1937 cells treated with sorafenib. **b** Transmission electron microscopy (TEM) of EVs showed vesicles with characteristic morphology and size, ranging from 50 to 150 nm in diameter. Scale bar, 100 nm. **c** Nanoparticle tracking analysis (NTA) showed heterogeneous size distribution profiles of the EVs derived from DMSO- or sorafenib-treated breast cancer cells.

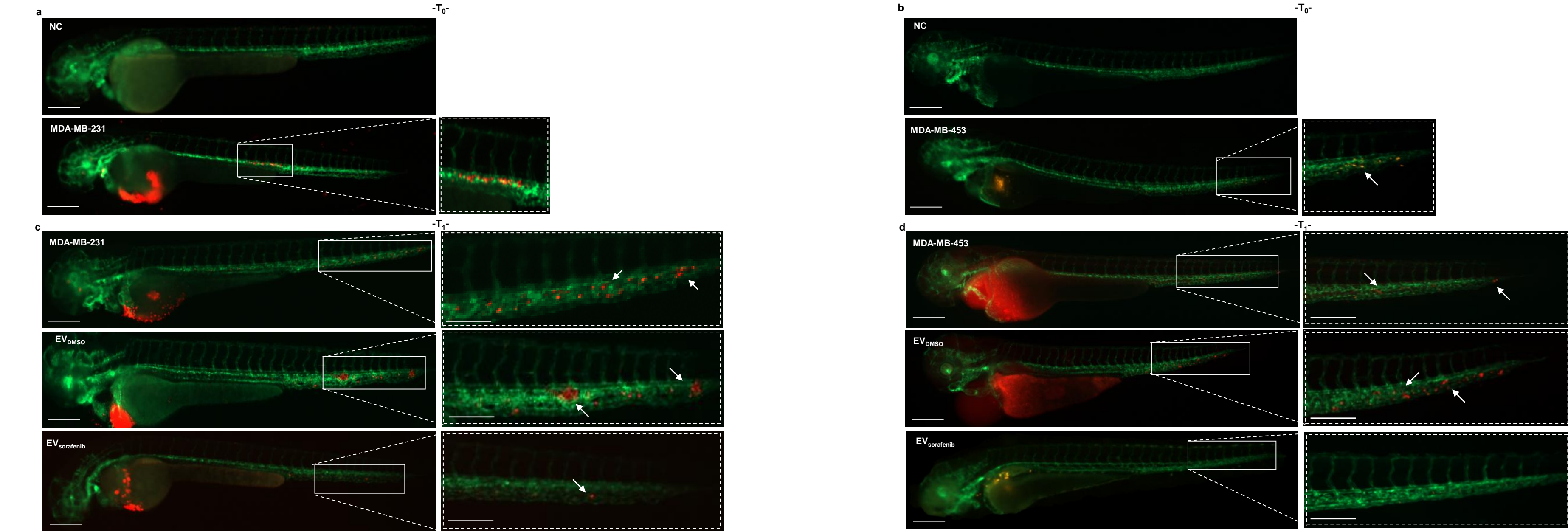


**EVs-based ncRNAs delivery to target breast cancer cells.** **a** Representative fluorescence microscopy images showing the uptake of MDA-MB-453 and MCF-7 derived extracellular EVs, labeled in red, by MDA-MB-231 and MDA-MB-453 recipient BC cells. Scale bars correspond to 30 μm for 63x magnification. **b** Expression levels of cellular miR-23b-3p, miR-126-3p, and GAS5 were determined in terms of copies/μL using ddPCR technology. Unpaired t-test was used to compare EV<sub>sorafenib</sub> treatment versus EV<sub>DMSO</sub>; \**p* < 0.05, \*\**p* < 0.01, \*\*\**p* < 0.001.

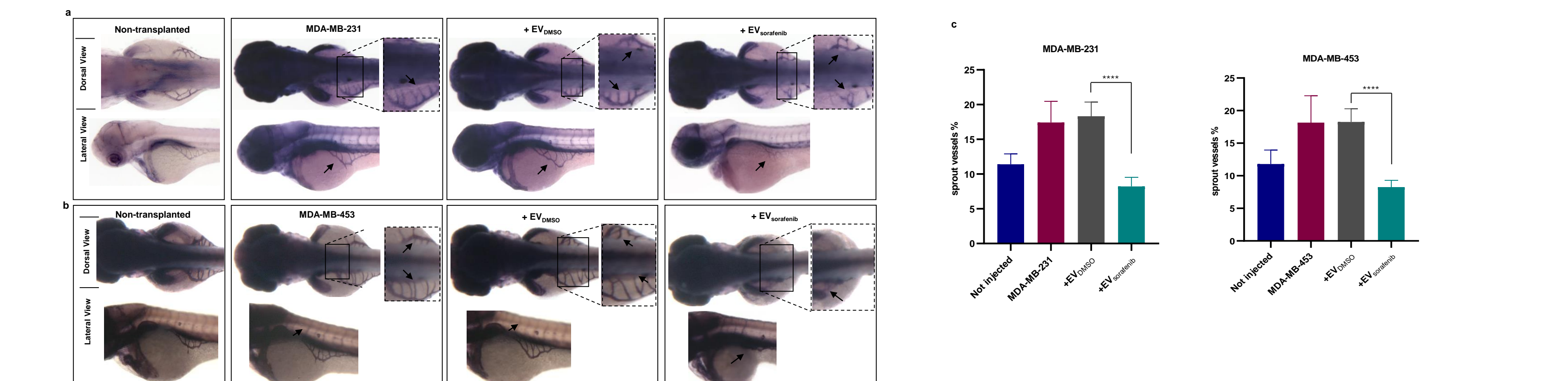
### In vivo



**Evs uptake in zebrafish.** **a** Fluorescent microscopy images of CM-Dil labeled EVs uptake by the recipient transgenic zebrafish line Tg(*kdrl*:EGFP). **b** Mortality analysis of embryos treated with EVs derived from MCF-7 and MDA-MB-453 at 72 hpf; data are representative of two replicates (*n* = 30 for each group) and are shown as the mean ± standard deviation; negative control embryos (NC) were exposed to 0.1% DMSO in fish water, while the positive control embryos (PC) were exposed to 3,4-DCA dissolved in fish water at a concentration of 3.74 mg/L; unpaired t-test was used; \**p* < 0.05, \*\**p* < 0.01, \*\*\*\**p* < 0.0001. Magnification 20x and 32x. Scale bars correspond to 500 μm.



**Effects of enriched EVs-based treatment on breast cancer xenografts at T<sub>0</sub> and T<sub>1</sub>.** Representative lateral view pictures of Tg(*kdrl*:EGFP) uninjected fish were used as negative control (NC); CM-Dil labeled a MDA-MB-231 and b MDA-MB-453 breast cancer (BC) cells were injected into the yolk sac of the 48 hpf zebrafish. Representative images of the zebrafish were acquired 2 hours post-injection (hpi) (T<sub>0</sub>); **c** - **d** at 24 hpi (T<sub>1</sub>), trunk and tail pictures were obtained, arrows indicate the formation of cancer cell clusters at the level of the tail. Scale bars correspond to 500 μm for magnification of 20x and 32x. **e** - **h** Quantification of the tumor area in the xenografts and the assessment of the tumor cell number in the tail were conducted at T<sub>0</sub> and T<sub>1</sub>. Data are representative of two replicates (*n* = 30 for each group) and are shown as the mean ± standard deviation; Unpaired t-test was used; \*\*\*\**p* < 0.0001.



**Xenotransplantation-induced angiogenesis in the zebrafish embryos.** The alkaline phosphatase assay was performed to assess the angiogenic potential of a MDA-MB-231 and b MDA-MB-453 cells, in embryos that were either untreated or treated, with enlargement of the sub-intestinal venous plexus (SIVP) region at 72 hpf. Magnification 63x. **c** The graphs represent the average number of SIVP branches at 72 hpf. Data are representative of two replicates (*n* = 30 for each group) and are shown as the mean ± standard deviation; Unpaired t-test was used; \*\*\*\**p* < 0.0001.